Chiral Hydrogels

DOI: 10.1002/anie.201403249

Control of Three-Dimensional Cell Adhesion by the Chirality of Nanofibers in Hydrogels**

*Guo-Feng Liu, Di Zhang, and Chuan-Liang Feng**

Abstract: *In the three-dimensional (3D) extracellular matrix (ECM), the influence of nanofiber chirality on cell behavior is very important; the helical nanofibrous structure is closely related to the relevant biological events. Herein, we describe the use of the two enantiomers of a 1,4-benzenedicarboxamide phenylalanine derivative as supramolecular gelators to investigate the influence of the chirality of nanofibers on cell adhesion and proliferation in three dimensions. It was found that left-handed helical nanofibers can increase cell adhesion and proliferation, whereas right-handed nanofibers have the opposite effect. These effects are ascribed to the mediation of the stereospecific interaction between chiral nanofibers and fibronectin. The results stress the crucial role of the chirality of nanofibers on cell-adhesion and cell-proliferation behavior in 3D environments.*

Chirality is one of the most distinctive biochemical signatures of life and has great influence on many biological events, for example, the maintenance of normal functions of living cells.[1] Pioneering research has revealed that cells can sense surface chiral molecules and show differential behavior on enantiomorphous surfaces.[2] Although of great significance in biomaterial and relevant biological studies, these studies have mainly been confined to the important role of molecular chirality on a two-dimensional (2D) surface, and a lot of questions remain.[3] Among them, how nanofibrous chirality influences cell behavior in the three-dimensional (3D) extracellular matrix (ECM) is especially important, since only the 3D ECM nanofibrous structure can really mimic the necessary biophysical environment for tissue engineering, and the helical nanofibrous structure is closely related to the relevant biological events;[1,2,4] however, this research area has not yet been explored.

Hydrogels have been widely used as a scaffold to provide 3D environments that are biophysically similar to the human ECM, which cannot be modeled by a conventional 2D matrix.[5] In this study, by employing the two enantiomers of a 1,4-benzenedicarboxamide phenylalanine derivative (D-PH and L-PH; Scheme 1) as supramolecular gelators, a novel hydrogel system with chiral nanofibrous structures was developed for cell culture (*l*-PH: left-handed nanofibers assembled from L-PH; *d*-PH: right-handed nanofibers assembled from D-PH). We show that a specific chirality of nanofibrous hydrogels can greatly enhance the cell adhesion and proliferation densities in a 3D environment. The cell densities of fibroblast cells (mouse embryonic fibroblast cell line, NIH 3T3) and endothelial cells (human umbilical vein endothelial cells, HUVECs) in the *l*-PH hydrogels were about twice as high as those in the *d*-type hydrogels, although the other physical and chemical properties of the *d*/*l*-PH hydrogels were similar. More interestingly, effective cell clusters could only form in *l*-PH hydrogels; this typical cell-growth character in three dimensions is crucially important for cell proliferation and differentiation in tissue engineering. An enzyme-linked immunosorbent assay (ELISA) study indicated that such differential cell behavior is largely mediated by the stereospecific interaction between chiral nanofibers of hydrogels and fibronectin (FN). This effect provides novel insight into the problem of controllable cell adhesion and proliferation in a 3D chiral environment, which is still a big challenge in tissue engineering and regenerative medicine.

A simple way to encapsulate cells into 3D hydrogels was developed by mixing the Dulbecco modified Eagle medium (DMEM) and cells into a concentrated solution of the gelator in dimethyl sulfoxide (DMSO; final DMSO concentration: 3.3%). In this way, self-supporting hydrogels were formed within several minutes (Scheme 1). With the merits of straightforward preparation, culture-medium response, and directional noncovalent interactions between gelators, the hydrogels exhibited unique properties superior to those of conventional polymeric hydrogels.[6] Circular dichroism (CD) and scanning electron microscopy (SEM) demonstrated that the *d*/*l*-PH hydrogels were constructed by opposite chiral nanofibers. However, the *d*/*l*-PH hydrogels presented almost the same chemical and physical properties, including the thickness and helical pitch of the nanofibers, pore size, and the stiffness of the hydrogels. Interestingly, cells cultured in *d*/*l*-PH gels showed significantly different behavior. The chirality of the nanofibers, and not the molecular chirality alone,[2a,g] is clearly responsible for these phenomena and plays a crucial role in the behavior of cells in the hydrogels.

The D/L-PH enantiomers were synthesized by a conventional liquid-phase reaction in high yield (see Scheme S1 and Figures S1 and S2 in the Supporting Information). The CD signals (Figure 1A) and optical-rotation values (see Table S1 in the Supporting Information) of the D-PH and L-PH enantiomers were equal in intensity and opposite in sign. The CD bands with λ_{max} values at 218 and 237 nm were due to

[*] G. F. Liu, Prof. D. Zhang, Prof. C. L. Feng
School of Materials Science and Engineering
Shanghai Jiaotong University
800 Dongchuan Road, Shanghai 200240 (P.R. China)
E-mail: clfeng@sjtu.edu.cn

[**] We thank the National Science Foundation of China (51173105, 51273111), the National Basic Research Program of China (973 Program 2012CB933803), and the Program for Professors of Special Appointment (Eastern Scholar) at Shanghai Institutions of Higher Learning, as well as the SRF for ROCS and SEM.

Supporting information for this article is available on the WWW under http://dx.doi.org/10.1002/anie.201403249.

 © 2014 Wiley-VCH Verlag GmbH & Co. KGaA, Weinheim

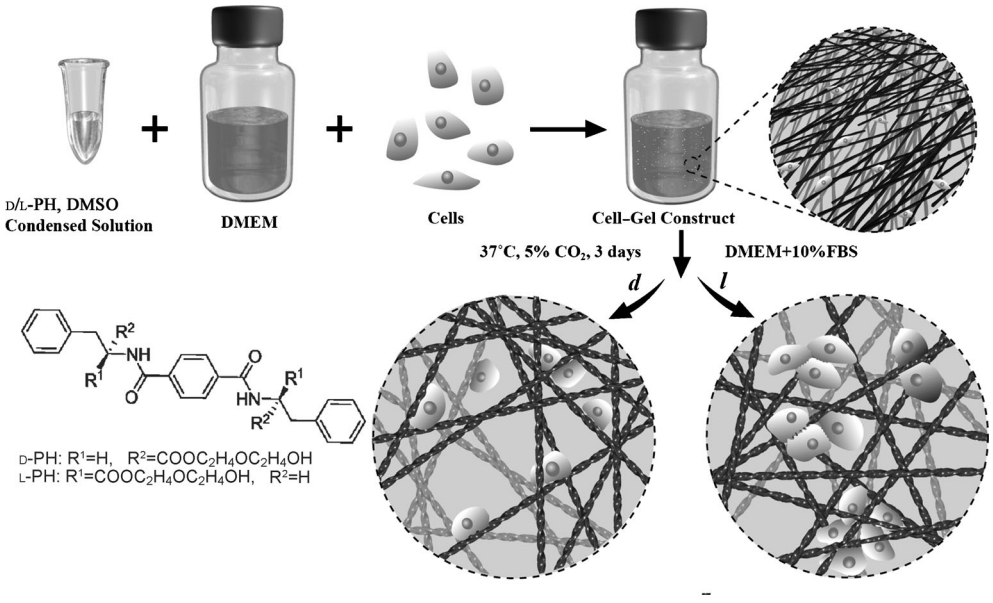

Scheme 1. Schematic representation of the culture of NIH 3T3 cells or HUVECs in supramolecular hydrogels and the different cell-adhesion and cell-proliferation behavior in the enantiomeric nanofibrous hydrogels (*d*: right-handed helical nanofibers; *l*: left-handed helical nanofibers). The molecular structure of the gelator enantiomers is shown.

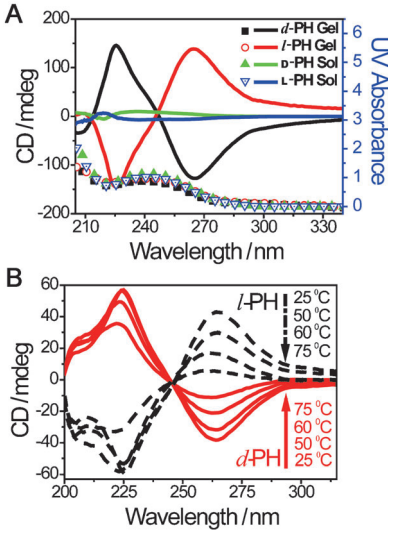

Figure 1. A) CD spectra (solid lines) of D-PH (green) and L-PH (blue) enantiomers in methanol and *d*-PH (black) and *l*-PH (red) hydrogels (2.0 mg mL^{-1}) in PBS, and the simultaneous UV/Vis spectra (symbols) of the enantiomers and hydrogels. B) Temperature-dependent CD spectra of *d*-PH (red solid line) and *l*-PH (black dotted line) hydrogels (1.0 mg mL^{-1}) with increasing temperature from 25 to 75 °C.

the amide carbonyl groups and phenyl group in the 1,4-benzenedicarboxamide, respectively.[7] The *d*/*l*-PH hydrogels showed significantly increased intensity (as compared with that of the *D*/*L*-PH enantiomers) and a perfect mirror-image relationship of the CD signals (Figure 1A; see also Figure S3a). Moreover, the spectral peaks for both gels shifted to 226 and 268 nm. No CD signals existed for a gel (*r*-PH) consisting of a racemic mixture of D-PH and L-PH gelators with a molar ratio of 1:1 (see Figure S3a). In this study, the effective concentration of the gelators in methanol (solution state) and in phosphate-buffered saline (PBS; gel state) were kept constant, as confirmed by UV/Vis spectra (Figure 1A; see also Figure S3a). In variable-temperature CD spectra of d/*l*-PH, the signal intensity decreased upon the transformation of the sample from a gel into a solution upon heating (Figure 1B). CD spectra (see Figure S3b) demonstrated that the self-assembly of D/L-PH reached equilibrium after about 1 h. All results revealed that the chirality of the gels was due to self-assembled aggregates or nanofibers and not individual gelator molecules.[8]

The morphology of the *d*/*l*-PH and *r*-PH hydrogels was characterized by SEM. The diameters of the pores in the hydrogels were found to lie in the range of tens of micrometers (Figure 2A,B; see also Figure S4b). The D-PH enantiomers self-assembled into right-handed helical nanofibers, and L-PH formed left-handed helical nanofibers (Figure 2C,D). The right-handed and left-handed helical nanofibers had similar diameters ((50 ± 10) nm) and helical pitch ((480 ± 40) nm). Intertwined and twisted *d*-PH and *l*-PH fibers with opposite helical morphology were also shown by transmission electron microscopy (TEM; see Figure S5) and atomic force microscopy (AFM; see Figure S6). Figure 2a–d and Figure 2e–h show photographic images of the free-standing hydrogels *d*-PH and *l*-PH, respectively, in PBS (see Figure S7 for all three types of hydrogels, including *r*-PH). When DMEM was added to the top of these hydrogels, dynamic exchange between DMEM and PBS occurred until the hydrogels became a homogeneous pink color. The lifetime of the stable hydrogels under these conditions was at least 20 days (Figure 2a–h; see also Figure S7). The stiffness of all hydrogels was also quite similar (storage modulus $G' \approx 7.4 \times 10^3$ Pa; loss modulus $G'' \approx 3.2 \times 10^3$ Pa), as measured with a rheometer.

To understand how the chirality of the 3D environment influences cell adhesion and proliferation, we prepared the *l*-PH, *d*-PH, and *r*-PH hydrogels with encapsulated NIH 3T3 cells and HUVECs. It was found that numerous HUVEC and NIH 3T3 cell clusters were evenly distributed in the *l*-PH hydrogel after culture for 3 days (Figure 3A, b,d). This result showed that the clusters formed as a result of cell proliferation rather than cell migration.[9] Interestingly, NIH 3T3 cells developed the typical elongated polygonal cobblestone morphology throughout the *l*-PH hydrogel (Figure 3A, d),

 © 2014 Wiley-VCH Verlag GmbH & Co. KGaA, Weinheim

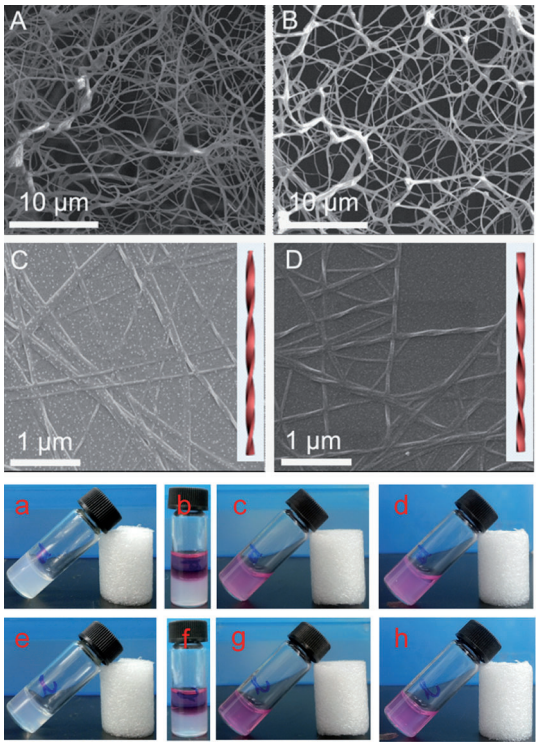

Figure 2. A, B) SEM images of *d*-PH (A) and *l*-PH (B) hydrogels after freeze-drying. C, D) SEM images of a *d*-PH xerogel with right-handed helical nanofibers (C) and an *l*-PH xerogel with left-handed helical nanofibers (D). Models of the helical nanofibers are also shown in (C, D). a–h) Photographic images of the free-standing *d*-PH (a–d) and *l*-PH (e–h) hydrogels in PBS before (a, e) and 0 min (b, f), 30 min (c, g), and 20 days (d, h) after the addition of an equal volume of DMEM on top of the hydrogel.

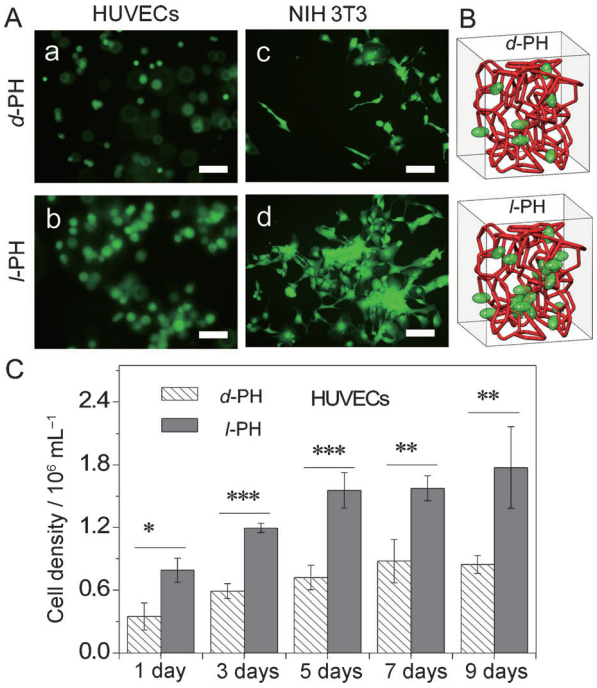

Figure 3. A) Fluorescence microscopy images of HUVECs (a, b) and NIH 3T3 cells (c, d) in *d*-PH and *l*-PH hydrogels after incubation for 3 days. Scale bar: 50 μm. B) Schematic representation of different cell-adhesion behaviors in the enantiomeric nanofibrous hydrogels. C) Quantitative data for HUVECs cultured in *d*-PH and *l*-PH hydrogels until day 9. $N = 3$; *, **, *** data show significant differences (ANOVA: $*p \le 0.05$, $** p \le 0.005$, $*** p \le 0.001$).

which indicated 3D proliferation behavior of the cells and a favorable interaction between the cells and *l*-type nanofibers.[10,11a] In contrast, only a small amount of cells were separately distributed in the *d*-PH hydrogels, and no polygonal cobblestone morphology was observed (Figures 3 A, a,c and 3 B). An intermediate adhesion and proliferation density was observed for the cells in *r*-PH hydrogels (see Figure S8 a). The proliferation densities in the *l*-PH hydrogels were calculated and found to be about double those in the *d*-PH hydrogels (Figure 3 C; see also Figure S8 c) throughout the culture period. The results demonstrate that cells cultured in 3D hydrogels constructed by *d*/*l*-PH chiral nanofibers showed different adhesion and proliferation behavior. High cell growth and proliferation density was observed in *l*-PH hydrogels, but not in *d*-PH hydrogels.

To prove that the different cell-adhesion and cell-proliferation behavior in the 3D environment is closely related to the chirality of the nanofibers, we seeded NIH 3T3 cells separately (ca. 2500 cells per well) on *d*-PH, *l*-PH, and *r*-PH hydrogel films and a polystyrene (PS) surface.[11] After incubation for 4 h, the quantity of adhered live cells on the *l*-PH nanofibrous films was 2.2 times as high as that on the *d*-PH films (see Table S2) and 1.3 times as high as that on *r*-PH films. After culture for 3 days, the cell-growth density was found to be proportional to the original adhesion density for each film (Figure 4 B; see also Figures S9 and S10), which suggested that a high adhesion density is crucial for achieving a high cell-proliferation density. Furthermore, most of the proliferated cells on *l*-PH films showed the elongated morphology, whereas cells on *d*-PH films mainly had a round morphology (Figure 4 A, a,b). To further prove the importance of the chirality of the nanofibers, we cultured cells on nonchiral PS films (see Figure S10). Both cell-adhesion and cell-growth density were found to be much lower than on *l*-PH films, but higher than on *d*-PH. Thus, the chirality of the nanofibers played an important role in regulating the interactions of the cells with the nanofibers. The good cytocompatibility of the nanofibers was also proved by a live–dead staining assay (see Figure S11).[9]

To examine whether the chirality effect was unique to the NIH 3T3 cell type, we seeded HUVECs on the different films (ca. 2000 cells per well). The results were similar to those observed with the NIH 3T3 cells: Both the cell-adhesion and cell-proliferation density on *l*-PH films was double that on *d*-PH films (see Table S3 and Figures S12 and S13). After culture for 5 days, many cells on *l*-PH films showed the elongated morphology, and most cells had a round shape on *d*-PH films (Figure 4). The results show that both types of cell behavior are greatly influenced by the chirality of the nanofibers. The *l*-PH nanofibers can increase cell adhesion and proliferation, whereas the *d*-PH nanofibers have the opposite effect. Thus, the different cell-adhesion and cell-proliferation behavior in 3D chiral hydrogels was mainly

 © 2014 Wiley-VCH Verlag GmbH & Co. KGaA, Weinheim

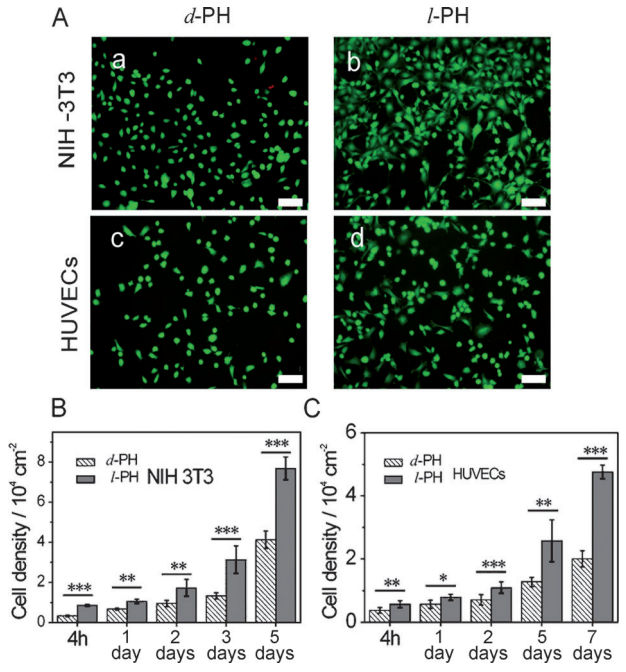

Figure 4. A) Fluorescence microscopy images of NIH 3T3 cells after culture for 3 days (a, b) and HUVECs after culture for 5 days (c, d) on *d*-PH and *l*-PH nanofibers. Scale bar: 100 μm. B, C) Quantitative data for NIH 3T3 cells (B) and HUVECs (C) on *d*-PH and *l*-PH films after incubation for 4 h, 1 day, 2 days, 3 days, 5 days, and 7 days. $N = 6$; *, **, *** data show significant differences (ANOVA: $*p \le 0.05$, $**$ $p \le 0.005$, $***$ $p \le 0.001$).

regulated by the chiral nanofibers, which could be recognized and differentiated by the cells.

The stereospecific interaction between cells and enantiomeric nanofibers was further studied by using fibronectin (FN), a well-known protein that promotes cell adhesion.[12] The adsorption behavior of FN on *d*-PH, *l*-PH, and *r*-PH nanofibrous films was analyzed by an ELISA assay. Figure 5A shows time-dependent curves of the amount of adsorbed FN on the films (see Figure S15a). After 40 min, the adsorption reached a plateau, and the amount of FN adsorbed on *l*-PH, *r*-PH, and *d*-PH films was calculated to be 0.114, 0.107, 0.093 ng cm^{-2}, respectively. A linear fit of the amount of FN versus time in the first 40 min is shown in Figure 5B (see also Figure S15b). The slope of the line represents the association constant of FN. The calculated constants were 0.1123 on the *l*-PH film, 0.0866 on the *r*-PH film, and 0.0527 on the *d*-PH film. These values suggest a fast adsorption rate of FN on *l*-PH films as a result of high selectivity of FN for the enantiomeric fibers. This assumption was further proved by investigating the adsorbed amount of FN on each of the enantiomeric matrices (see Figure S16). Thus, it can reasonably be speculated that the chirality of the nanofibers is recognized by the cells through stereospecific interactions between the chiral fibers and FN in three dimensions. Interactions with different fibers (*l*-PH or *d*-PH) may release different signals to the cells and result in different cell/substrate interactions.[1b,13]

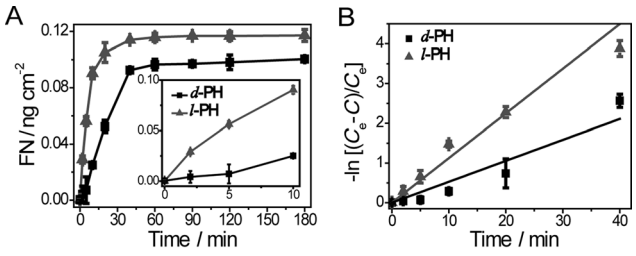

Figure 5. A) Time-dependent adsorption of FN on *d*-PH (squares) and *l*-PH (triangles) nanofibrous films. The *y* axis shows the amount (ng) of FN adsorbed per square centimeter of film. Inset: Adsorption of FN on *d*/*l*-PH nanofibrous films from 0 to 10 min. B) Linearization of the amount of FN on *d*-PH and *l*-PH films according to pseudo-first-order kinetics.

As discussed above, the stereospecific interaction between the cells and the chiral nanofibers is not a unique but a common effect that should be applicable to different cell types. Cells have a stronger interaction with *l*-type nanofibers through stereospecific recognition between cells and nanofibers. It is thus considered that the design of enantiomorphous environments may be a novel advantageous direction for biomaterials design. This approach is complementary to existing strategies to control cell density for tissue engineering.

In conclusion, the chirality of nanofibrous structures has great influence on cell adhesion and proliferation in the 3D ECM. The cells were found to adhere and grow significantly more densely in *l*-type than in *d*-type 3D microenvironments. Further study on the interaction between FN and the enantiomeric nanofibers provided evidence for a protein-mediated process to explain this effect. These results provide important insight for the development of a new generation of 3D matrices to control cell-adhesion and cell-proliferation density. They stress the key role of the chirality of nanostructures for materials design and offer a novel way to achieve high-density cell growth in the 3D ECM. Owing to its generality, it can reasonably be anticipated that the use of this effect, in combination with other properties of materials, for example, stiffness, may lead to the appearance of some new applications, such as therapeutic uses of stem cells.[14]

Experimental Section

Materials and characterization: D/L-phenylalanine methyl ester hydrochloride, 1,4-benzenedicarbonyl dichloride, and diglycol were purchased from Aladdin Chemicals. The detailed synthesis of gelators D/L-PH is shown in Scheme S1. NMR spectroscopic experiments were performed by using a Bruker Advance III 400 instrument operated at 400 MHz. FABMS spectra were obtained with a JEOL JMS 700 mass spectrometer. CD kinetic spectra were collected on a JASCO J-815 CD spectrometer with a bandwidth of 1.0 nm. Variable-temperature CD spectroscopy was carried out by increasing the temperature in steps of 5 °C. The nanofibrous hydrogels were characterized by SEM with a FEI Quanta 250 microscope, by TEM with a Tecnai G2 Spirit BioTWIN microscope (FEI, USA), and by AFM with an E-Sweep microscope (Seiko, Japan). The cells were quantified by using the program Image J.

Hydrogel preparation: DMSO (500 μL) was added to a vial containing the gelator (30 mg). DMEM (15 mL) was added to the resulting solution to form a hydrogel (gelator concentration: 2.0 mg mL^{-1}). The critical gel concentration (CGC) of D/L-PH was

 © 2014 Wiley-VCH Verlag GmbH & Co. KGaA, Weinheim

0.5 mg mL^{-1}, and the CGC of a 1:1 mixture of the two enantiomers (*r*-PH gel) was 1.0 mg mL^{-1}.

Cell culture: The HUVEC cell strain was originally purchased from American Type Culture Collection (ATCC, Rockville, MD, USA); NIH 3T3 was a gift from the School of Biomedical Engineering of SJTU. For 2D and 3D cell culture, see the Supporting Information.

Live–dead staining assay and CCK8: A fluorescence live–dead staining assay (Invitrogen) was used to visualize the proportion of viable and nonviable cells. The CCK8 assay was carried out with 10% (v/v) WTS-8, and the absorbance was measured by ELISA (Infinite M200 PRO, Tecan) at 450 nm (see the Supporting Information).

FN adsorption: FN measurements (absorbance at 450 nm) were carried out by ELISA. A quantity of 100 μL of a standard solution of FN (400 pg mL^{-1}) was added to each well coated with hydrogels, and the plates were incubated at 37 °C in an atmosphere containing 5% CO_2.

Received: March 12, 2014
Published online: June 10, 2014

Keywords: cell adhesion · chirality · enantiomers · hydrogelators · nanofibers

[1] a) D. Hanein, B. Geiger, L. Addadi, *Science* **1994**, *263*, 1413 – 1416; b) R. M. Hazen, D. S. Sholl, *Nat. Mater.* **2003**, *2*, 367 – 374.

[2] a) T. L. Sun, D. Han, K. Rhemann, L. F. Chi, H. Fuchs, *J. Am. Chem. Soc.* **2007**, *129*, 1496 – 1497; b) T. L. Sun, G. Qing, B. Su, L. Jiang, *Chem. Soc. Rev.* **2011**, *40*, 2909 – 2921; c) M. X. Zhang, G. Y. Qing, T. L. Sun, *Chem. Soc. Rev.* **2012**, *41*, 1972 – 1984; d) X. Wang, H. Gan, T. L. Sun, B. L. Su, H. Fuchs, D. Vestweber, S. Butz, *Soft Matter* **2010**, *6*, 3851; e) X. Wang, H. Gan, M. X. Zhang, T. L. Sun, *Langmuir* **2012**, *28*, 2791 – 2798; f) F. Zhou, L. Yuan, D. Li, H. Huang, T. L. Sun, H. Chen, *Colloids Surf. B* **2012**, *90*, 97 – 101; g) J. El-Gindi, K. Benson, L. De Cola, H. J. Galla, N. S. Kehr, *Angew. Chem.* **2012**, *124*, 3776 – 3780; *Angew. Chem. Int. Ed.* **2012**, *51*, 3716 – 3720; h) D. Bandyopadhyay, D. Prashar, Y. Y. Luk, *Chem. Commun.* **2011**, *47*, 6165 – 6167; i) D. Bandyopadhyay, D. Prashar, Y. Y. Luk, *Langmuir* **2011**, *27*, 6124 – 6131; j) X. Yao, Y. Hu, B. Cao, R. Peng, J. D. Ding, *Biomaterials* **2013**, *34*, 9001 – 9009.

[3] a) K. J. Tang, H. Gan, Y. Li, L. F. Chi, T. L. Sun, H. Fuchs, *J. Am. Chem. Soc.* **2008**, *130*, 11284 – 11285; b) G. Y. Qing, X. Wang, H. Fuchs, T. L. Sun, *J. Am. Chem. Soc.* **2009**, *131*, 8370; c) H. Gan, K. J. Tang, T. L. Sun, M. Hirtz, Y. Li, L. F. Chi, S. Butz, H. Fuchs, *Angew. Chem.* **2009**, *121*, 5386 – 5390; *Angew. Chem. Int. Ed.* **2009**, *48*, 5282 – 5286; d) X. Wang, H. Gan, T. L. Sun, *Adv. Funct. Mater.* **2011**, *21*, 3276 – 3281; e) G. Qing, X. Shan, W. Chen, Z. Lv, P. Xiong, T. Sun, *Angew. Chem.* **2014**, *126*, 2156 – 2161; *Angew. Chem. Int. Ed.* **2014**, *53*, 2124 – 2129; f) Y. Li, Y. Zhou, H. Y. Wang, S. Perrett, Y. Zhao, Z. Tang, G. Nie, *Angew. Chem.* **2011**, *123*, 5982 – 5986; *Angew. Chem. Int. Ed.* **2011**, *50*, 5860 – 5864; g) Y. Wang, J. Xu, H. Y. Chen, *Chem. Soc. Rev.* **2013**, *42*, 2930; h) L. C. Cheng, X. M. Jiang, J. Wang, C. Y. Chen, R. S. Liu, *Nanoscale* **2013**, *5*, 3547 – 3569.

[4] a) Z. L. Luo, S. G. Zhang, *Chem. Soc. Rev.* **2012**, *41*, 4736 – 4754; b) Z. L. Luo, Y. Y. Yue, Y. F. Zhang, X. Yuan, J. P. Gong, L. L. Wang, B. He, Z. Liu, Y. L. Sun, J. Liu, M. F. Hu, J. Zheng, *Biomaterials* **2013**, *34*, 4902 – 4913.

[5] a) M. C. Cushing, K. S. Anseth, *Science* **2007**, *316*, 1133 – 1134; b) C. L. Feng, X. Q. Dou, D. Zhang, H. Schonherr, *Macromol. Rapid Commun.* **2012**, *33*, 1535 – 1541; c) X. Q. Dou, P. Li, D. Zhang, C. L. Feng, *J. Mater. Chem. B* **2013**, *1*, 3562 – 3568.

[6] a) S. G. Zhang, *Nat. Biotechnol.* **2003**, *21*, 1171 – 1178; b) R. M. Capito, H. S. Azevedo, Y. S. Velichko, A. Mata, S. I. Stupp, *Science* **2008**, *319*, 1812 – 1816; c) A. M. Kloxin, A. M. Kasko, C. N. Salinas, K. S. Anseth, *Science* **2009**, *324*, 59 – 63; d) P. Terech, R. G. Weiss, *Chem. Rev.* **1997**, *97*, 3133 – 3160; e) L. E. Buerkle, S. J. Rowan, *Chem. Soc. Rev.* **2012**, *41*, 6089 – 6102.

[7] a) A. R. Hirst, D. K. Smith, M. C. Feiters, H. P. M. Geurts, *Chem. Eur. J.* **2004**, *10*, 5901 – 5910; b) W. Edwards, D. K. Smith, *J. Am. Chem. Soc.* **2014**, *136*, 1116 – 1124.

[8] a) D. K. Smith, *Chem. Soc. Rev.* **2009**, *38*, 684 – 694; b) A. Friggeri, C. van der Pol, K. J. C. van Bommel, A. Heeres, M. C. A. Stuart, B. L. Feringa, J. van Esch, *Chem. Eur. J.* **2005**, *11*, 5353 – 5361; c) L. Brunsveld, H. Zhang, M. Glasbeek, J. A. J. M. Vekemans, E. W. Meijer, *J. Am. Chem. Soc.* **2000**, *122*, 6175 – 6182; d) K. Murata, M. Aoki, T. Suzuki, T. Harada, H. Kawabata, T. Komori, F. Ohseto, K. Ueda, S. Shinkai, *J. Am. Chem. Soc.* **1994**, *116*, 6664 – 6676.

[9] C. S. Szot, C. F. Buchanan, J. W. Freeman, M. N. Rylander, *Biomaterials* **2011**, *32*, 7905 – 7912.

[10] M. Zhou, A. M. Smith, A. K. Das, N. W. Hodson, R. F. Collins, R. V. Ulijn, J. E. Gough, *Biomaterials* **2009**, *30*, 2523 – 2530.

[11] a) J. K. Kretsinger, L. A. Haines, B. Ozbas, D. J. Pochan, J. P. Schneider, *Biomaterials* **2005**, *26*, 5177 – 5186; b) Y. F. Tian, J. M. Devgun, J. H. Collier, *Soft Matter* **2011**, *7*, 6005 – 6011.

[12] A. Dekker, K. Reitsma, T. Beugeling, A. Bantjes, J. Feijen, W. G. van Aken, *Biomaterials* **1991**, *12*, 130 – 138.

[13] a) R. M. Hazen, T. R. Filley, G. A. Goodfriend, *Proc. Natl. Acad. Sci. USA* **2001**, *98*, 5487 – 5490; b) V. Vogel, M. Sheetz, *Nat. Rev. Mol. Cell Biol.* **2006**, *7*, 265 – 275.

[14] A. J. Engler, S. Sen, H. L. Sweeney, D. E. Discher, *Cell* **2006**, *126*, 677 – 689.

 © 2014 Wiley-VCH Verlag GmbH & Co. KGaA, Weinheim